Electrochemical and Spectral Characterization of the Reduction Steps of μ-Oxo-bis(iron tetraphenylporphyrin) Dimer in Dimethylformamide

Karl M. Kadish,*[1a] Gary Larson,[1a] Doris Lexa,[1b] and Michel Momenteau[1b]

Contribution from the Department of Chemistry, California State University, Fullerton, California 92634, and Laboratoire de Biophysique du Museum National d'Histoire Naturelle, 75005 Paris, France. *Received April 27, 1974*

Abstract: The electrochemical reduction of μ-oxo-bis(iron(III) tetraphenylporphyrin) has been found to proceed *via* several discrete steps to yield, as final product, a species characterized as the first ring reduction of iron(I) tetraphenylporphyrin. All steps have been examined by esr, visible spectroscopy, cyclic voltammetry, and coulometry. The initial reduction yields, first, and intermediate paramagnetic ferric–ferrous dimer, then a ferrous dimer, and, finally, two distinctly different complexes of ferrous monomers, which appear to be in equilibrium with each other. Further reduction yields two forms of iron(I), both of which are characterized by a split Soret band. An overall mechanism is proposed based on the results of product identification after each reduction. To our knowledge this study presents the first spectral evidence for a mixed ferrous–ferric porphyrin dimer.

The structure and electron transfer properties of various iron porphyrins have received considerable attention due to their importance in biological electron exchange reactions. These studies have involved electrochemical, chemical, and spectral determinations in both aqueous and nonaqueous media.[2-18] In aqueous solutions iron porphyrins are known to dimerize.[19] Bednarski and Jordan investigated iron protoporphyrin IX in basic solution and observed that the ferric species was always dimeric, while the ferrous form was either dimeric or monomeric depending on pH.[20] Further electrochemical studies by Kadish and Jordan[21] showed that the overall two-electron reduction of dimeric iron protoporphyrin IX proceeded *via* an initial one-electron transfer yielding a mixed Fe(II)–Fe(III) species. This assignment was based solely on electrochemical data and no spectral evidence was presented.

Our interest in this paper is in the electroreduction mechanism of iron tetraphenylporphyrin dimers in nonaqueous media. Two types of reductions, those at the central iron atom and those at porphyrin ring, can be observed. In order to distinguish the reduction products, we will use the following notation to identify the complexes: the species $[Fe^{III}TPP]^+$ indicates the iron(III) α,β,γ,δ-tetraphenylporphyrin with a total charge of plus one, $[Fe^{II}TPP]^0$ indicates the neutral iron(II) complex, $[Fe^{I}TPP]^-$ indicates the d^7 iron(I) tetraphenylporphyrin, with an overall charge on the complex of minus one, and $[Fe^{I}TPP]^{2-}$ corresponds to the first ring reduction product of iron(I) tetraphenylporphyrin. $(FeTPP)_2O$ corresponds to an oxo bridged dimer of iron(III) tetraphenylporphyrin.

Recent crystallographic studies[22,23] have shown that this latter species exists as the μ-oxo-bis(iron tetraphenylporphyrin) dimer where the porphyrins are held together by a single oxygen ion bridging the metal atoms. This structure for tetraphenylporphyrin as well as other μ-oxo-bridged iron(III) dimers has been confirmed by ir spectroscopy[24,25] and nmr techniques.[26-28]

Visible and esr spectroscopy and magnetic susceptibility measurements have shown the formation of a d^7 iron(I), $[Fe^{I}TPP]^-$, as a chemical reduction product of $(FeTPP)_2O$ in THF.[29] Electrochemical reduction of monomeric $Fe^{III}TPPCl$ also produces $[Fe^{I}TPP]^-$ and proceeds in three discrete single-electron transfer steps yielding $[Fe^{II}TPP]^0$, $[Fe^{I}TPP]^-$, and finally $[Fe^{I}TPP]^{2-}$, which is the product of the first ring reduction.[18] All of these reductions are reversible in DMF, THF, and DMSO[2a,18] and the electron transfer rates for the first two reductions of $Fe^{III}TPPCl$ have been calculated as being of the order of 10^{-2} cm²/sec in DMSO.[2a]

It was indicated by Cohen, *et al.*,[29] that chemical reduction of $(Fe^{III}TPP)_2O$ proceeded in several steps, although no products other than $[Fe^{I}TPP]^-$ were characterized. This paper reports the overall electrochemical reduction mechanism for the conversion of $(Fe^{III}TPP)_2O$ to $[Fe^{I}TPP]^{2-}$ at an electrode surface. Structural assignments are based on optical and esr spectra as well as electrochemical data.

Experimental Section

I. Chemicals. Reagent grade chemicals were used throughout. Dried dimethylformamide (DMF, Mallinckrodt) was vacuum distilled immediately before use. Dried, recrystallized tetraethylammonium perchlorate (TEAP, Eastman Organic Chemicals), at a concentration of 0.1 *M*, was used as supporting electrolyte in all solutions. Tetrabutylammonium hydroxide (Bu_4NOH, 25% in methanol, MCB) was used as obtained. $Fe^{III}TPPCl$ and $(FeTPP)_2O$ were prepared according to published procedures.[22,30]

II. Polarography and Cyclic Voltammetry. Polarographic measurements were made on Princeton Applied Research Models 170, 173, and 174 electrochemistry systems utilizing a three-electrode geometry. The working electrode consisted of either a dropping mercury electrode (DME), a hanging mercury drop electrode of Kemula type design (Model E-410, Metrohn), or a platinum button electrode of surface area 0.25 mm².

A commercial calomel electrode was used as the reference electrode and a platinum wire as the auxiliary electrode. The reference electrode was separated from the bulk of the solution by a bridge filled with DMF and supporting electrolyte. Solutions in the bridge were changed periodically. This arrangement, thus, prevented aqueous contamination from entering the cell *via* the calomel electrode. The electrolysis cell was a Brinkman Model EA 875-5. Total volume utilized was 5–10 ml, and porphyrin concentrations were between 10^{-3} and 10^{-4} *M*. Linear and cyclic sweep rates were varied between 0.01 and 10 V/sec. At the higher scan rates, ir drop was corrected for by the use of a positive feedback system which was built into the Model 170 and 173 polarograph. All scans above 0.2 V/sec were measured on a Model 5103N Tektronix storage oscilloscope, provided with a camera attachment. The overall number of electrons (faradays per mole of electroreduced monomer) was determined by controlled potential coulometry. A Princeton Applied Research Model 173 potentiostat was used to control the potential at which experiments were run. Electronic integration of the current time curve was achieved by means of a PAR Model 179 integrator, which yielded a voltage output that was recorded on an X-Y recorder. The coulometric cell was similar to that used for cyclic voltammetry. A large coiled platinum wire served as the

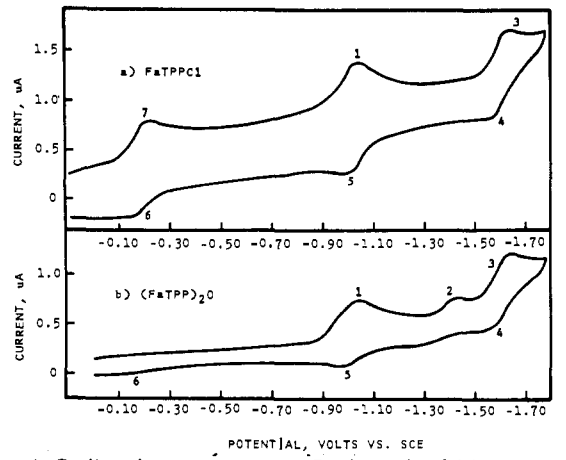

Figure 1. Cyclic voltammograms at a Pt electrode of (a) 8.63×10^{-4} *M* FeTPPCl and (b) 7.69×10^{-4} *M* $(FeTPP)_2O$ in DMF, 0.1 *M* TEAP. Scan rate = 0.1 V/sec.

anode and was separated from the cathodic compartment by means of a fritted disk which fitted into the center of the cell. A stirred mercury pool of area ≈7 cm^2 served as the cathode and a saturated calomel electrode was the reference electrode. Stirring of the solution was achieved by means of a magnetic stirring bar positioned atop the mercury pool and actuated by a motor beneath the cell. Deaeration of the solution was performed before commencing the experiment and a stream of high purity nitrogen was passed throughout. All experiments were carried out in a controlled temperature room of 20 ± 0.5° and potentials are reported with respect to the saturated calomel electrode (sce).

III. Optical and Electron Spin Resonance Spectroscopy. Constant voltage electrolysis was carried out in quartz cells described in a previous publication.[18] The electrolysis was followed optically using a Cary 15 spectrophotometer and checked magnetically on a Varian X-band esr spectrometer. The magnetic field strength was computed from the nuclear resonance frequency of a proton probe located next to the cavity (Varian F 8 A magnetometer). This frequency was determined with a Hewlett Packard 5245L frequency counter. The microwave frequency was measured with a calibrated wave meter. Samples were frozen at 77°K in liquid N_2.

Results

Polarography and Cyclic Voltammetry. The electrochemical reduction of $(FeTPP)_2O$ proceeds in several discrete steps without destroying the porphyrin ring. In Figure 1 is shown a typical cyclic voltammogram of $(FeTPP)_2O$ obtained in DMF. Also shown for comparison in this figure is the reduction of monomeric FeTPPCl in the same solvent. In order to investigate each reduction process separately and evaluate subsequent chemical reactions following electron transfer, cyclic voltammograms were taken at various potential sweep ranges. The potential was initially set at 0.0 V and scanned in a cathodic direction. For FeTPPCl a reversible reduction was invariably observed at −0.19 V, which can be assigned to the transition

$$[Fe^{III}TPP]^+ \xrightarrow{e^-} [Fe^{II}TPP]^0$$

However, in contrast to the facile reduction of FeTPPCl, no reaction was observed for $(FeTPP)_2O$ in any range of scans up to cathodic potentials of at least −0.9 V.

When the scan was extended to −1.2 V, peaks 1, 5, and 6 of Figure 1 were obtained. Peak 6 gave a current which was about 10% of the other peaks and was ill-defined. The potential sweep rate was then varied over the range of 0.002–2 V/sec. The inherent advantage of cyclic voltammetry is that the scan rates can be varied over a large range and, in so doing, one can often resolve overlapping chemical or electrochemical processes which may be indistinguishable in the time interval of normal dc polarography.[31]

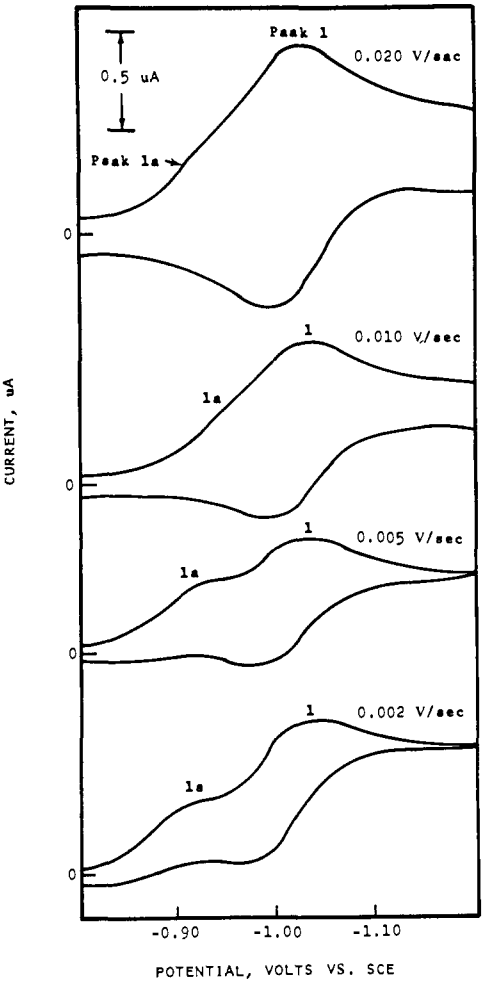

Figure 2. Cyclic voltammograms at a hmde of 3×10^{-4} *M* $(FeTTP)_2O$ showing resolution of overlapping reduction peaks with decreasing scan rate. TEAP is 0.1 *M* in DMF. v = 0.020, 0.010, 0.005, and 0.002 V/sec.

The effect of scan rate variation on $(FeTPP)_2O$ is shown in Figure 2. As the scan was decreased, peak 1 broadened until, at the lowest rate of 0.002 V/sec, two distinct reductions were evident due to the anodic displacement of a new peak from the shoulder of peak 1. This peak is labeled peak 1a in Figure 2 and was only observed at scan rates less than 0.05 V/sec. In no case was a corresponding oxidation observed for this reduction.

When the cathodic scan was further extended, a diffusion controlled reduction peak at *ca.* −1.38 V was obtained corresponding to the transfer of a single electron (peak 2, Figure 1). The potential of this peak was a function of sweep rate. Experimental plots of peak potential *vs.* scan rate yielded a cathodic shift of 0.032 V per tenfold increase in scan rate over the range of 0.05–10 V/sec, while the peak shape always remained that of a reversible one-electron transfer ($E_p - E_{p_{1/2}} = 0.057$ V). No corresponding oxidation was ever observed, and peaks 1 and 5 remained unchanged. At scan rates lower than 0.05 V/sec, the magnitude of peak 2 decreased until, at the lowest sweep, it disappeared altogether.

Controlled Potential Electrolysis. In order to identify the products of each individual reduction step, $(FeTPP)_2O$ was reduced at several controlled potentials and a polarogram was recorded after total electrolysis. The initial dc polarogram of $(FeTPP)_2O$ before electrolysis is shown in Figure 3a. The potential was then set at −1.2 V. This is on the plateau of the first reduction wave (which was shown to be

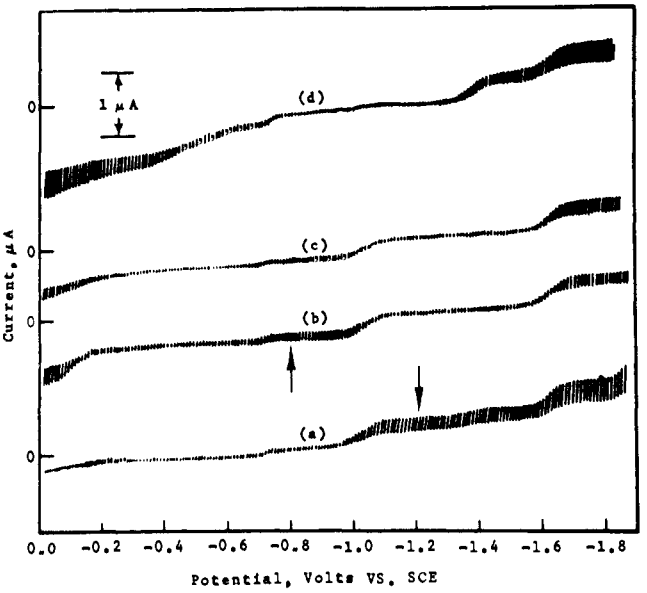

Figure 3. Polarograms obtained during controlled potential electrolysis of $(FeTPP)_2O$: (a) $(FeTPP)_2O$ in DMF, 0.1 *M* TEAP; (b) after complete electrolysis at −1.2 V to produce $[Fe^{I}TPP]^-$; (c) during reoxidation at −0.8 V to give a mixture of $[Fe^{II}TPP]^0$ and $[Fe^{I}TPP]^-$; (d) after addition of 10^{-3} *M* Bu_4NOH to $(FeTPP)_2O$. The wave at −0.5 V is attributed to mercury oxidation and was observed in the absence of porphyrin to increase in current as a function of hydroxide concentration.

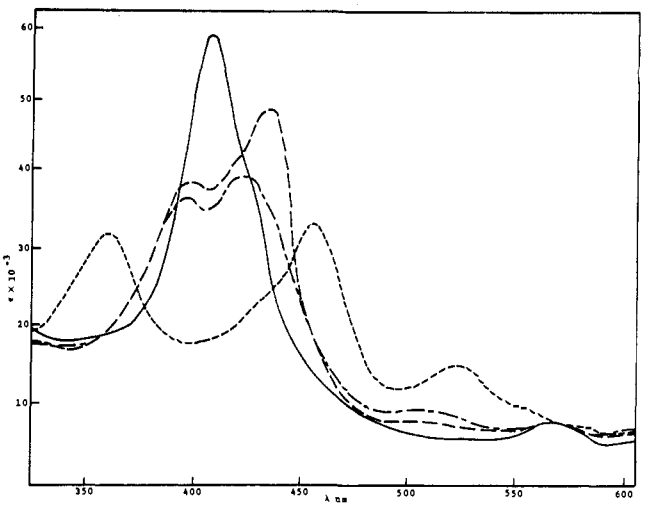

Figure 4. Optical studies of the electrolysis products of $(FeTPP)_2O$ in DMF, 0.1 *M* TEAP: $(FeTPP)_2O$ before electrolysis (——); during controlled potential reduction at −0.93 V (——); after complete electrolysis at −0.93 V (— — —); after controlled potential reduction at −1.4 V to yield $[Fe^{I}TPP]^-$, form A (- - - -).

composed of two overlapping processes), but 0.20 V anodic of the second reduction wave. Controlled potential electrolysis at this potential yielded a decrease in both the reduction wave at −1.03 and −1.38 V and a concomitant increase in the oxidation wave at −1.03 V. This is shown in Figure 3b. Reoxidation of this solution at −0.80 V (Figure 3c) gave a polarogram possessing a reversible composite wave at −1.03 V with no wave observed at −1.38 V. A wave at −0.19 V for $[Fe^{II}TPP]^0 \rightarrow [Fe^{III}TPP]^+$ was seen. As will be suggested, the wave at −1.38 V can be attributed to the reduction of $[Fe^{II}TPPOH]^-$ or $[Fe^{II}TPPO]^{2-}$ formed from cleavage of $(FeTPP)_2O$ after reduction to the ferrous form. The wave at −1.0 V has been characterized in an earlier study as belonging to the reversible reduction of $[Fe^{II}TPP]^0$.[18]

In order to investigate the apparent equilibrium between the Fe(II) compound reduced at −1.0 V and that at −1.38 V, tetrabutylammonium hydroxide, Bu_4NOH (10^{-3} *M*), was added to solutions of $(FeTPP)_2O$ to produce quantities of OH^- which might serve as a coordination ligand to the iron. If the more cathodic reduction at −1.38 V was due to an iron(II) hydroxide complex, one might shift the equilibrium on additions of OH^- and, consequently, observe a decrease in the concentration of uncomplexed form reduced at −1.03 V and an increase in the complexed form reduced at −1.38 V. The results of OH^- addition are shown in Figure 3d. The initial wave at −1.03 V disappeared and was replaced by another wave of about equal current intensity at −1.38 V. Throughout the studies, no change was observed in the most cathodic reduction which invariably occurred at −1.61 V. Identical results were also obtained when OH^- was added to FeTPPCl in DMF.

Optical Spectra. Before electrolysis, the well-characterized[18,29] spectrum of $(FeTPP)_2O$ was obtained (Figure 4a). On reduction at −0.93 V, this was first transformed to that spectra identified as $Fe^{II}TPP$[18] (Soret band maximum at 428 nm), as well as small amounts of a second compound, characterized by a Soret band at λ 438 nm. No isosbestic points were observed. In addition, $[Fe^{I}TPP]^-$ was also obtained at this potential. This agrees with the electrochemical results, which indicate the initial two-electron reduction of $(FeTPP)_2O$ occurs *via* several overlapping steps yielding $[Fe^{I}TPP]^-$. This latter species designated as form B is characterized by a split Soret band (λ 420 and 390 nm) and is one of two distinct spectral forms of $[Fe^{I}TPP]^-$.[18] The second form (form A) was produced by reduction of $(FeTPP)_2O$ at −1.4 V and yielded a split Soret band at λ 457 and 362 nm. The spectra are displayed in Figures 4 and 5.

Hydroxide was then added to fresh solutions, and the spectra were recorded after controlled potential reduction at −0.93 and −1.1 V (Figure 5). Additions of 10^{-3} *M* Bu_4NOH to $(FeTPP)_2O$ produced no change in the initial spectra. However, under these experimental conditions, electrolysis at −0.93 V produced only a single reduction product (Soret band at λ 432 nm) with well-defined isosbestic points observed (Figure 5a). This latter spectrum was identical with that produced by addition of Bu_4NOH to monomeric $[Fe^{II}TPP]^0$, which had been generated from FeTPPCl by hydrogen reduction on palladium. The order of magnitude of the ϵ_{max} is comparable to that of the Soret band for the high spin $Fe^{II}TPP$ previously characterized.[18] At this potential, no $[Fe^{I}TPP]^-$ of either form was observed nor was the transient species at λ 438 nm present. After complete electrolysis, the potential was changed to −1.1 V and the iron(II) complex again reduced at controlled potential.

Continued electrolysis at −1.1 V yielded a transformation of the iron(II) hydroxide spectrum to the split Soret band spectrum of iron(I), form B (λ 420 and 390 nm), with definite isosbestic points again being obtained (Figure 5b). When the porphyrin was reduced at −1.4 V, iron(I), form A was obtained (λ 457 and 362 nm).

Electron Spin Resonance. An esr spectrum was not observed for the starting material, $(FeTPP)_2O$. Reduction at −0.93 V gave rise to an intermediate species whose esr spectrum at 77°K showed one asymmetric line characterizing an anisotropic *g* (g_1 = 1.95). This is shown in Figure 6. If the solution was heated and refrozen after partial electrolysis, no signal was observed, indicating a disappearance of the paramagnetic species from solution.

When the electrolysis of $(FeTPP)_2O$ was carried out at −1.1 V, the esr spectra initially showed both the intermedi-

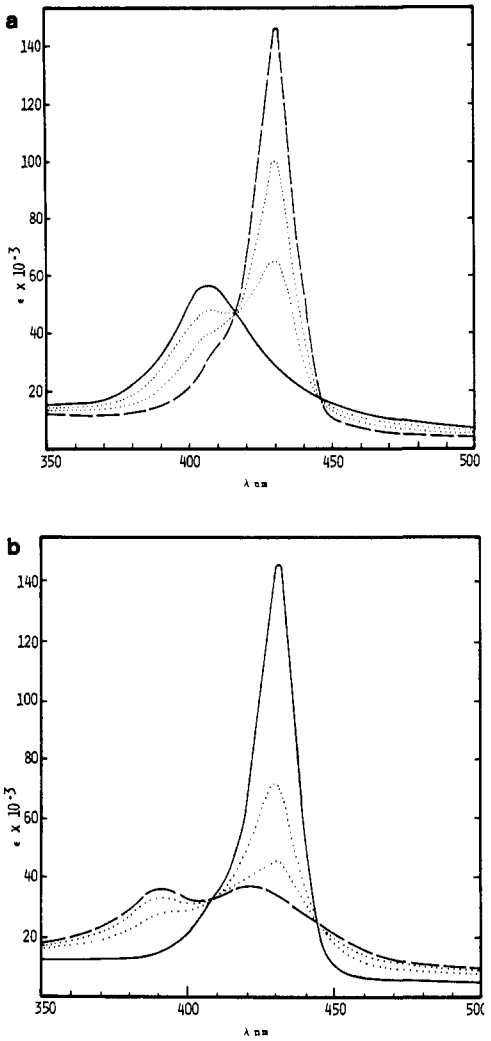

Figure 5. Electrolysis products of $(FeTPP)_2O$ after controlled potential electrolysis in 10^{-3} *M* Bu_4NOH: (a) $(FeTPP)_2O$ before electrolysis (——); after complete reduction at −0.93 V to yield $[Fe^{II}TPPOH]^-$ (——); intermediate spectra (·····); (b) $[Fe^{II}TPPOH]^-$ (——); after electrolysis at −1.1 V to yield $[Fe^{I}TPP]^-$, form B (——); intermediate spectra (·····).

ate (g = 1.95) and the stable product $[Fe^{I}TPP]^-$ (g_1 = 1.93 and g_2 = 2.30). This is shown in Figure 6. Total electrolysis of this potential produced only a single spectrum of $[Fe^{I}TPP]^-$. A splitting of the g = 2.30 line was observed. This same splitting at g = 2.30 was also observed for $[Fe^{I}TPP]^-$ generated by reduction of monomeric $FeTPPCl$.[18]

Electrolysis at −1.30 V produced an esr spectrum identical with that generated at −1.1 V and the intermediate was not observed during reduction. However, if the electrolysis was stopped before complete reduction, the intermediate paramagnetic species at g = 1.95 could be obtained by agitation of the cell, which, presumably, allowed the generated $[Fe^{I}TPP]^-$ to react with unreduced $(FeTPP)_2O$, thereby, producing the Fe^{II}-O-Fe^{III} paramagnetic intermediate.

In the presence of Bu_4NOH, the intermediate radical was not observed on reduction of $(FeTPP)_2O$. This agrees with the optical spectra which show a well-defined isosbestic point, indicating a single equilibrium between $(FeTPP)_2O$ and $[Fe^{II}TPPOH]^-$. Again, however, the radical could be produced by mixing reduced $[Fe^{I}TPP]^-$ with $(FeTPP)_2O$.

Discussion of Results

Based on the data, the reduction of $(Fe^{III}TPP)_2O$ in the absence of added OH^- can be accounted for by the following mechanism.

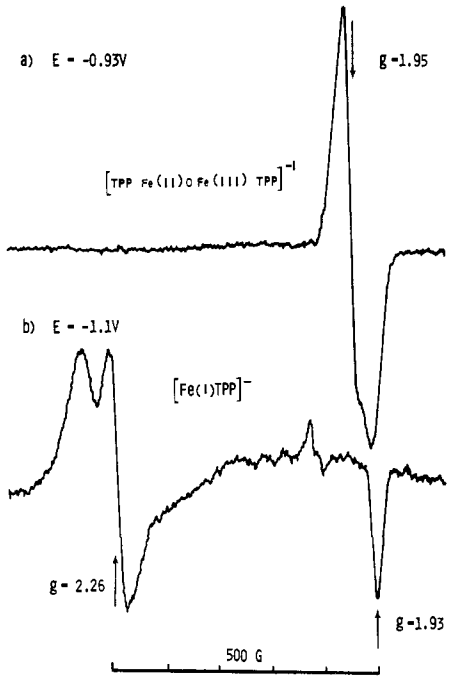

Figure 6. Esr spectra at 77°K in dimethylformamide obtained during the electrolysis of $(FeTPP)_2O$: (a) E = −0.93 V showing appearance of the intermediate paramagnetic species; (b) E = −1.1 V showing characteristic spectra of $[Fe^{I}TPP]^-$. A weak organic radical is seen at g = 2. It has not been identified, but could be assigned to some nonmetallic tetraphenylporphyrin as impurity.

$$[TPPFe^{III}\text{-}O\text{-}Fe^{III}TPP]^0 \xrightleftharpoons{+e^-} [TPPFe^{III}\text{-}O\text{-}Fe^{II}TPP]^- \qquad E_{1/2} \approx -0.93\ V \quad (1a)$$

$$[TPPFe^{III}\text{-}O\text{-}Fe^{II}TPP]^- \xrightleftharpoons{+e^-} [TPPFe^{II}\text{-}O\text{-}Fe^{II}TPP]^{2-} \qquad E_{1/2} \leq -0.93\ V \quad (1b)$$

$$[TPPFe^{II}\text{-}O\text{-}Fe^{II}TPP]^{2-} \xrightarrow{H^+} [Fe^{II}TPP]^0 + [Fe^{II}TPPOH]^-$$

$$[Fe^{II}TPP]^0 \xrightleftharpoons{+e^-} [Fe^{I}TPP]^- \qquad E_{1/2} = -1.03\ V \quad (2)$$

$$[Fe^{II}TPPOH]^- \xrightleftharpoons{+e^-} [Fe^{I}TPPOH]^{2-} \xrightarrow{H^+} [Fe^{I}TPP]^- + H_2O \qquad E_{1/2} \approx -1.38\ V \quad (3)$$

$$[Fe^{I}TPP]^- \xrightleftharpoons{+e^-} [Fe^{I}TPP]^{2-} \qquad E_{1/2} = -1.61\ V \quad (4)$$

The initial reduction of dimeric $(Fe^{III}TPP)_2O$ to monomeric $Fe^{II}TPP$ can be written in three separate steps yielding first an intermediate ferric-ferrous dimer, then a ferrous dimer, and, finally, two distinctly different complexes of ferrous monomers.

The hypothesis for the formation of Fe^{III}-O-Fe^{II} can be deduced from the esr spectra. The initial $(Fe^{III}TPP)_2O$ does not yield an esr signal at either 77°K or room temperature due to an antiferromagnetic coupling between the S = ½ metal ions. This spin state has been suggested by both susceptibility measurements[32] and Mössbauer studies.[33] $Fe^{II}TPP$ with electronic configuration $3d^6$ can be found in several spin states (S = 0, 1, or 2), according to the nature of the axial ligands,[34,35] and also does not yield an esr signal at 77°K. As seen in Figure 6, reduction of $(FeTPP)_2O$ to

$Fe^{II}TPP$ gave rise to an intermediate species, whose esr signal at 77°K showed one asymmetric line, characterizing an anisotropic g (g_1 = 1.95). This paramagnetic species is only stable at 77°K and is assigned to a mixed ferrous-ferric dimer produced by the addition of a single electron to $(FeTPP)_2O$. The possibility that the intermediate paramagnetic species seen upon reduction is $[Fe^{III}TPP]^+$, resulting from a splitting of the dimer, seems unlikely since high spin iron porphyrin would be produced and the characteristic signal[10] at g = 6 was not seen. It also cannot be identified as any other Fe(III) species obtained from the addition of one or two ligands to the Z coordination position of the iron yielding either high or low spin compounds. On the other hand, this asymmetrical esr radical observed at g = 1.95 cannot be identified with the symmetrical radical (g = 2.09) observed by Cohen, *et al.*,[29] when pyridine is added to $[Fe^{I}TPP]^-$ in THF. In our experiments the radical at g = 1.95 was never present after total reduction to $[Fe^{I}TPP]^-$, but could be produced by oxidation of $[Fe^{I}TPP]^-$, either by oxygen or mixing with unreacted ferric dimer. It is not stable in the presence of tetrabutylammonium hydroxide.

The electrochemical data provides no evidence for the postulated sequence of separate single electron transfer steps preceding the dimer cleavage (reaction 1a-b). It is clear from the esr spectra that a paramagnetic intermediate is formed in the reduction of $(FeTPP)_2O$. Thus, the addition of a second electron to the postulated intermediate $[TPPFe^{III}\text{-}O\text{-}Fe^{II}TPP]^-$ would be needed to obtain the ferrous reduction product, which would show no esr spectra.

One can also envisage a dissociation of the mixed dimer sandwiched between two single-electron transfers. This could be written as

$$[TPPFe^{III}\text{-}O\text{-}Fe^{III}TPP]^0 \xrightarrow{+e^-} [Fe^{III}TPP\text{-}O\text{-}Fe^{II}TPP]^-$$
$$E = -0.93\ V \qquad \downarrow H^+$$
$$[Fe^{III}TPPOH]^0 + [Fe^{II}TPP]^0$$
$$e^- \downarrow \quad E \leq -0.93\ V$$
$$[Fe^{II}TPPOH]^-$$

The $[Fe^{III}TPPOH]^0$ formed would be immediately reduced at −0.93 V and, thus, electrochemically this might appear very similar to the reaction sequence 1a, b. If the second transfer were rapid enough, the characteristic signal for $[Fe^{III}TPP]^+$ at g = 6 might not be detected due to a low steady state concentration. The possibility of a disproportionation mechanism also cannot be ruled out as an alternate possibility to reaction 1b. Such a sequence has been postulated for a somewhat different iron porphyrin dimer.[21] In our system, studies of disproportionation, based on changes in the current voltage curve with scan rate, could not be investigated due to the limited range of experimentally obtainable sweep rates at which peaks 1 and 1a did not overlap.

Further indications of a dimer cleavage to yield $[Fe^{II}TPP]^0$ come from Figure 2, where a resolution of the two overlapping reduction peaks (peaks 1 and 1a) was obtained by changing the potential sweep rate. The direction of the peak 1a shift (anodic with decreasing scan) can be accounted for by a chemical reaction, following a fast transfer of electrons.[31] This chemical reaction would be a cleaving of the ferrous prophyrin dimer to produce monomeric $[Fe^{II}TPP]^0$, which was observed by optical spectra during controlled potential reduction at −0.93 V. That $[Fe^{II}TPP]^0$ is generated as a reduction product after −0.93 V is immediately evident from a comparison of the cyclic voltammograms of $Fe^{III}TPPCl$ and $(Fe^{III}TPP)_2O$ (Figure 1). Both species yield identical reduction peaks 1 and 3 at E_p = −1.06 and −1.61 V and oxidation peaks 4 and 5 at −1.55 and −1.00 V. These processes have been previously characterized[17,18] by electrochemical and optical spectra as corresponding to the successive reduction of monomeric $[Fe^{II}TPP]^0$ to $[Fe^{I}TPP]^-$ and then to $[Fe^{I}TPP]^{2-}$ by single-electron transfers.

We have indicated that two distinct forms of ferrous monomer were observed upon reduction. One of them, $[Fe^{II}TPP]^0$, is immediately reduced to $[Fe^{I}TPP]^-$ at −1.03 V while the second, written as $[Fe^{II}TPPOH]^-$, is not reducible before −1.38 V and also yields $[Fe^{I}TPP]^-$ as a final product. The equilibrium between these forms can be represented in the following manner.

$$[Fe^{II}TPP]^0 + OH^- \rightleftharpoons [Fe^{II}TPPOH]^-$$
$$+e^- \downarrow\uparrow E_{1/2} = -1.03\ V \qquad +e^- \downarrow\uparrow E_{1/2} = -1.38\ V$$
$$[Fe^{I}TPP]^- \qquad [Fe^{I}TPPOH]^{2-}$$
$$\downarrow$$
$$[Fe^{I}TPP]^- + OH^-$$

Since $[Fe^{II}TPP]^0$ is more easily reduced than $[Fe^{II}TPPOH]^-$, reduction at −1.1 V will cause a shift of the equilibrium to the left and only $[Fe^{I}TPP]^-$ will be produced.

This was verified by controlled potential electrolysis as shown in Figure 3. According to the scheme, reduction of $[Fe^{II}TPPOH]^-$ also gives $[Fe^{I}TPP]^-$ as final product after dissociation of $[Fe^{I}TPPOH]^{2-}$. This was confirmed by cyclic voltammetry (Figure 1) where reduction at −1.38 V yielded a reverse oxidation at −1.03 V. In addition, the observed 0.032 V cathodic displacement of the reduction peak, with tenfold change in scan rate, agrees well with the theoretical 0.030 V predicted for a chemical reaction following electron transfer, as postulated in reaction 3. No oxidation peak was observed, supporting this mechanism.

In the presence of excess OH^-, the equilibrium will shift to the right yielding $[Fe^{II}TPPOH]^-$. This is shown in Figure 3d where addition of OH^- to $(FeTPP)_2O$ produced a decrease of the wave at −1.03 V and an increase in the wave at −1.38 V. Identical results were obtained upon addition of OH^- to FeTPPCl. Again, only $[Fe^{I}TPP]^-$ is produced on electroreduction at −1.1 V, despite the fact that $[Fe^{II}TPPOH]^-$ is the predominant species in solution.

Complexation of metal ions usually shifts the reduction potential to more negative values.[36] In fact, studies of reduction potentials have shown a cathodic shift of 0.30–0.50 V on complexation of iron with OH^- in aqueous solution.[37] Similar shifts in half-wave potential have been seen when comparing heme iron with a water coordination at the Z position and that of a OH^- ligand attachment.[38] Thus, our observed difference of 0.4 V between the two ferrous forms can be explained on the basis of a OH^- ligand attachment. Further proof of this assignment comes from optical spectra taken in the presence of tetrabutylammonium hydroxide.

In the presence of excess hydroxide, reduction of $(FeTPP)_2O$ yields mainly the intermediate $[Fe^{II}TPPOH]^-$ which has been shown to be in equilibrium with the uncomplexed $[Fe^{II}TPP]^0$. Optical absorption spectra of $[Fe^{II}TPPOH]^-$, generated at −0.93 V in the presence of hydroxide (Figure 5a), show a Soret band indicative of monomeric $[Fe^{II}TPP]^0$, but displaced from λ 428 to 432 nm. The same spectra could be obtained by titrating $Fe^{II}TPP$ with hydroxide. This was done to verify by separate experiments the existence of $[Fe^{II}TPPOH]^-$. FeTPPCl was reduced by hydrogen on palladium and the generated $Fe^{II}TPP$ was spectrophotometrically titrated with Bu_4NOH. The resulting spectrum was similar to that ob-

tained after reduction of $(FeTPP)_2O$ at −0.93 V, in the presence of Bu_4NOH. DMF is known to decompose in the presence of Bu_4NOH. This reaction, however, is slow at concentrations less than 10^{-2} *M*, and measurements can easily be made before decomposition. When the concentration of Bu_4NOH was increased, the decomposition of DMF was significant, and another complex with the generated dimethylamine was observed (λ 445, 572, and 615 nm). This was verified in a separate experiment with dimethylamine itself. Thus, the observed shift of 4 nm from λ 428 to λ 432 nm can be accounted for by a replacement of a molecule of solvent by one OH^- in the *Z* coordination position of the iron.[17] Similar small wavelength shifts have been observed in our laboratories when Cl^- is substituted for F^- in solutions of $Fe^{II}TPP$ and iron(II) deuterioporphyrin.

We have observed in this investigation two forms of $Fe^{I}TPP$. Form A, which was generated by reduction of $(FeTPP)_2O$ at −1.4 V, has a split Soret band maximum at 457 and 362 nm while form B was generated from the same species at −1.1 V and also yields a split Soret band at λ 420 and 390 nm. (These spectra were identical with those observed for the reduction of monomeric FeTPPCl in either THF or DMF as reported in a previous investigation.[18]) The spectral maximum agrees very closely with those reported by Cohen[29] for the chemical reduction of $(FeTPP)_2O$. Here reduction by Na·Hg yielded first a red compound identified as $[Fe^{I}TPP]^-$ which converted to a yellow-green compound and finally to a green compound which can be identified as the anion radical $[Fe^{I}TPP]^{2-}$. The visible peak maximum of Fe(I), form B previously recorded in DMF[18] at 510, 580, and 660 nm, agrees closely with those of 535, 575, and 675 nm for the yellow-green compound in THF.[29] For B is the only species produced on electroreduction at −1.1 V. In marked contrast the red Fe(I) compound, which appears first on chemical reduction of $(FeTPP)_2O$, has peaks at 540 and 605 nm and corresponds to our Fe(I), spectral form A produced at $E = -1.4$ V. Electrochemical reduction at −1.4 V is very similar to chemical reduction with Na·Hg in that, at this potential, $[Fe^{II}TPPOH]^-$ can be directly reduced without prior conversion to the more easily reducible form $[Fe^{II}TPP]^0$.

Comparison of our Fe(I) esr spectra generated by electroreduction at $E = -1.1$ V (Figure 6) and that produced by chemical reduction shows a splitting of the former spectra at $g = 2.30$. The answer to this apparent discrepancy between chemical and electrochemical reduction can be found in comparing the strong reducing strength of Na·Hg with that of electroreduction (−1.1 V). Chemical reduction with Na·Hg yields as final product the anion radical $[Fe^{I}TPP]^{2-}$ while electrochemical reduction at −1.1 V produces $[Fe^{I}TPP]^-$ as the final reduction product. As previously indicated,[29] chemical reduction of $(FeTPP)_2O$ yields first a red Fe(I) compound which converts to an unidentified yellow-green compound before forming the final green anion radical, $[Fe^{I}TPP]^{2-}$.

We would like to suggest that the split esr spectrum of Fe(I) corresponds to either the yellow-green compound, form B, or mixture of both forms B and A. Both of these Fe(I) esr spectra are very similar and have an identical $g = 1.93$ component. The equilibrium laws are temperature dependent, and depending on the ability to freeze the sample somewhat different solution conditions may result on changing from room temperature to 77°K. It was noted in an earlier study[18] that the esr spectra of $[Fe^{I}TPP]^-$ was not invariant and, depending on solvent conditions, the component at $g = 2.30$ varied between a singlet and a doublet. The splitting at $g = 2.30$ does not appear to be due to an anisotropy of the *g* due to distortion of the porphyrin plane but rather appears to genuinely reflect the presence of two separate forms of Fe(I). This is consistent with the electrochemical and spectral results reported in this paper which show the existence of two Fe(I) species in equilibrium.

Stability of the Dimeric Forms. The great difference between the half-wave potential for the reduction of iron(III) to iron(II) in FeTPPCl and $(FeTPP)_2O$ shows the greatly enhanced stability of this latter compound. Its reduction mechanism can be compared to that proposed by Kadish and Jordan[21] for aqueous iron protoporphyrin IX dimer. Both dimers appear to proceed *via* an initial single-electron transfer yielding a mixed ferrous–ferric species. However, in aqueous solution there is no evidence for or against the existence of an oxo bridge and it is thus not clear whether we are comparing reactions of identical dimeric structures.

According to Lemberg and Legge,[39] dimerization in aqueous solution may occur *via* a double propionate linkage (with attachment to the central iron of the other porphyrin and *vice versa*). Walter[40] has suggested coupling through a water bridge between the iron centers. More recent electrochemical studies by Bednarski and Jordan have pointed to the existence of two dimeric forms as a function of pH.[20] At pH >13 the dimer linkage was postulated as a double propionate linkage while at lower pH a water bridge was present.

In aqueous solution iron complexes may also exist as dihydroxo-bridged complexes where the two hydroxyl groups are bonded to each iron.[41-43] The structural issue can often be resolved on the basis of infrared properties of oxo bridges as described by Cotton and Wing.[44] In nonaqueous media the iron oxo bridge is well known and has been shown to be present in $(FeTPP)_2O$.[7,22,29] Initial studies of an oxo-bridged protoporphyrin IX dimer in nonaqueous media show that this species is similar in spectra and redox behavior to $(FeTPP)_2O$ but quite different from aqueous dimeric iron protoporphyrin IX.[45] This seems to indicate that distinctly different dimeric forms are present in an aqueous and nonaqueous environment.

It is possible to represent the ferric dimer by several mesomeric forms

$$[TPPFe^{III}\,O^{2-}\,Fe^{III}TPP]^0 \longleftrightarrow$$

I

$$[TPPFe^{III}\,O^{-}\,Fe^{II}TPP]^0 \longleftrightarrow [TPPFe^{II}-O-Fe^{II}TPP]^0$$

II III

The antiferromagnetic coupling[30] between the two iron ions is indicative of a direct electronic interaction but the stereochemical structure of the complex has shown that it is mainly in the ionic form I.[22,23] When the ferric dimer is reduced, the resonance energy coming from the electrostatic interaction must decrease.

Mesomeric resonance of the monoreduced intermediate represented as

$$[TPPFe^{II}\,O^{2-}\,Fe^{III}TPP]^- \longleftrightarrow [TPPFe^{III}\,O^{2-}\,Fe^{II}TPP]^-$$

would tend to stabilize a ferrous–ferric dimer but this structure would not favor a ferrous–ferrous oxo form and would thus explain its dissociation (reaction 1b) after the addition of two electrons.

In the presence of hydroxide, decomposition of the mixed ferric–ferrous dimer appears to be related to further axial coordination by OH^-. The mechanism of cleavage of the oxo bridge is related to the concentration of water and pH of solution as has been shown in aqueous media by other authors.[22,23] Indeed, the ferric dimer is not stable in acidic solutions and in DMF is reduced to ferrous monomer by H_2 on Pd.[17]

We have proposed in this study the existence of an Fe(III), Fe(II) μ-oxo bridged dimer. To our knowledge, this study presents the first spectral evidence for a mixed fer-

rous-ferric porphyrin dimer. This is not unique to tetraphenylporphyrin but has been observed in deuterioporphyrin, aetioporphyrin, protoporphyrin IX, and other similar dimeric species. In the latter species, marked differences in stability exist depending on the ring substitution positions. Results of this will be presented in a separate study.

Acknowledgments. The support of a California State University, Fullerton Faculty Grant is gratefully acknowledged. We would also like to thank J. Mispelter for his helpful discussions and M. Reix and B. Loock for technical aid.

References and Notes

(1) (a) California State University. (b) Laboratoire de Biophysique du Museum National d'Histoire Naturelle.
(2) (a) K. M. Kadish and D. G. Davis, *Ann. N.Y. Acad. Sci.*, **206**, 495 (1973); (b) J. H. Fuhrhop, K. M. Kadish, and D. G. Davis, *J. Amer. Chem. Soc.*, **95**, 5140 (1973).
(3) D. G. Davis and R. F. Martin, *J. Amer. Chem. Soc.*, **88**, 1365 (1966).
(4) D. G. Davis and D. J. Orgeron, *Anal. Chem.*, **38**, 179 (1966).
(5) H. R. Gygax and J. Jordan, *Discuss. Faraday Soc.*, **45**, 227 (1968).
(6) R. H. Felton, G. S. Owen, D. Dolphin, A. Forman, D. C. Berg, and J. Fajer, *Ann. N.Y. Acad. Sci.*, **206**, 504 (1973).
(7) R. H. Felton, G. S. Owen, D. Dolphin, and J. Fajer, *J. Amer. Chem. Soc.*, **93**, 6332 (1971).
(8) R. H. Felton, J. Fajer, D. C. Berg, and D. Dolphin, *J. Amer. Chem. Soc.*, **92**, 3451 (1970).
(9) S. R. Betso, M. H. Klapper, and L. B. Anderson, *J. Amer. Chem. Soc.*, **94**, 8197 (1972).
(10) A. Wolberg and J. Manassen, *J. Amer. Chem. Soc.*, **92**, 2982 (1970).
(11) J. Peisach, W. E. Blumberg, and A. Adler, *Ann. N.Y. Acad. Sci.*, **206**, 310 (1973).
(12) G. S. Wilson and B. P. Neri, *Ann. N.Y. Acad. Sci.*, **206**, 568 (1973).
(13) G. N. LaMar and F. A. Walker, *J. Amer. Chem. Soc.*, **95**, 6950 (1973).
(14) G. N. LaMar and F. A. Walker, *J. Amer. Chem. Soc.*, **95**, 1782 (1973).
(15) G. N. LaMar, G. R. Eaton, R. H. Holm, and F. A. Walker, *J. Amer. Chem. Soc.*, **95**, 63 (1973).
(16) M. Momenteau, *Biochim. Biophys. Acta*, **304**, 814 (1973).
(17) D. Lexa, Thesis, The University of Paris, 1972.
(18) D. Lexa, M. Momenteau, and J. Mispelter, *Biochim. Biophys. Acta*, **338**, 151 (1974).
(19) J. E. Falk, "Porphyrins and Metalloporphyrins," Elsevier, New York, N.Y., 1964.
(20) T. M. Bednarski and J. Jordan, *J. Amer. Chem. Soc.*, **89**, 1552 (1967).
(21) K. M. Kadish and J. Jordan, *Anal. Lett.*, **3**, 133 (1970).
(22) E. B. Fleischer and T. S. Srivastava, *J. Amer. Chem. Soc.*, **91**, 2403 (1969).
(23) A. B. Hoffman, D. M. Collins, V. W. Day, E. B. Fleischer, T. S. Srivastava, and J. C. Hoard, *J. Amer. Chem. Soc.*, **94**, 3620 (1972).
(24) I. A. Cohen, *J. Amer. Chem. Soc.*, **91**, 1980 (1969).
(25) S. B. Brown, P. Jones, and I. R. Lantzke, *Nature (London)*, **223**, 960 (1969).
(26) W. M. Reiff, G. J. Long, and W. A. Baker, *J. Amer. Chem. Soc.*, **90**, 6347 (1968).
(27) P. D. W. Boyd and T. D. Smith, *Inorg. Chem.*, **10**, 2041 (1971).
(28) M. Wicholas, R. Mustacich, and D. Jayne, *J. Amer. Chem. Soc.*, **94**, 4518 (1972).
(29) I. A. Cohen, D. Ostfeld, and B. Lichtenstein, *J. Amer. Chem. Soc.*, **94**, 4522 (1972).
(30) C. Maricondi, W. Swift, and D. K. Straub, *J. Amer. Chem. Soc.*, **91**, 5206 (1969).
(31) (a) R. S. Nicholson and I. Shain, *Anal. Chem.*, **36**, 706 (1964); (b) R. N. Adams, "Electrochemistry at Solid Electrodes," Marcel Dekker, New York, N.Y., 1969.
(32) T. H. Moss, R. H. Lilienthal, C. Moleski, G. A. Smyth, M. McDonnel, and W. S. Caughey, *J. Chem. Soc., Chem. Commun.*, 263 (1972).
(33) M. A. Torrens, D. K. Straub, and L. M. Epstein, *J. Amer. Chem. Soc.*, **94**, 4160 (1972).
(34) H. Kobayashi, M. Shimizu, and I. Fujita, *Bull. Chem. Soc. Jap.*, **43**, 8 (1970).
(35) J. P. Collman and C. E. Reed, *J. Amer. Chem. Soc.*, **95**, 2048 (1973).
(36) I. M. Kolthoff and J. J. Lingane, "Polarography," 2nd ed, Interscience, New York, N.Y., 1952.
(37) M. C. Day, Jr., and J. Selbin, "Theoretical Inorganic Chemistry," 2nd ed, Reinhold, New York, N.Y., 1969.
(38) W. M. Clark, "Oxidation Reduction Potentials of Organic Systems," Williams and Wilkins, Baltimore, Md., 1960.
(39) R. Lemberg and J. W. Legge, "Haematin Compounds and Bile Pigments," Interscience, New York, N.Y., 1949.
(40) R. I. Walter, *J. Biol. Chem.*, **196**, 151 (1951).
(41) H. Wendt, *Inorg. Chem.*, **8**, 1527 (1969).
(42) H. Schugar, C. Walling, R. Jones, and H. B. Gray, *J. Amer. Chem. Soc.*, **89**, 3712 (1967).
(43) H. Schugar, G. R. Rossman, and H. B. Gray, *J. Amer. Chem. Soc.*, **91**, 4564 (1969).
(44) F. A. Cotton and R. M. Wing, *Inorg. Chem.*, **4**, 867 (1965).
(45) K. M. Kadish, unpublished results.

Hydrate–Carbonyl Equilibrium in the Complex Pentacyano(4-formylpyridine)iron(II) and the Kinetics of Some Related Electron Exchange Reactions[1a]

Henrique E. Toma[1b] and John M. Malin*[1c]

Contribution from the Instituto de Quimica, Universidade de Sao Paulo, Sao Paulo, Brazil, and the Department of Chemistry, University of Missouri, Columbia, Missouri 65201. *Received July 1, 1974.*

Abstract: The influence of the pentacyanoiron(II) substituent on the ligand hydration equilibrium in the complex pentacyano(4-formylpyridine)iron(II) has been studied spectrophotometrically by following the shifts with temperature of the $\pi^* \leftarrow d\pi$ electron transfer bands in the visible–uv region. In the complex, the hydration constant, 0.48, measured at 37°, pH 7, and $\mu = 0.10$ *M* $LiClO_4$, is lower than those reported both for free and for protonated 4-formylpyridine, yet higher than that known for the pentaammine(4-formylpyridine)ruthenium(II) species. The observation is attributable to moderate stabilization of the aldehydo, relative to the hydrated form of the ligand by back-donation from the $Fe(CN)_5^{3-}$ moiety. The first-order rate constant for the hydration process is 2.4×10^{-2} sec^{-1} at 25°, pH 4.7, and $\mu = 0.10$. An investigation of the kinetics of electron transfer between pentacyano(pyridine)iron(II) and -(III) with hexacyanoiron(III) and -(II) has also been performed. Using the Marcus theory, the rate constant for self-exchange in pentacyano(pyridine)iron(II) and -(III) is calculated to be 2.4×10^6 M^{-1} sec^{-1} at 25°.

The properties of metal ions are modified by synthesizing complexes among which the charge, coordination geometry, or ligand field strength varies. Special significance arises when a ubiquitous ion, *e.g.*, iron(II), can be made to mimic the reactivity of the interesting but costly ruthenium(II). Octahedral, low spin complexes of the latter have attracted considerable attention because of their ability to interact with suitable ligands *via* metal-to-ligand back-donation.[2-6]